Biophysical Journal, Volume *111*

Supplemental Information

The Secreted Signaling Protein Wnt3 Is Associated with Membrane Domains In Vivo: A SPIM-FCS Study

Xue Wen Ng, Cathleen Teh, Vladimir Korzh, and Thorsten Wohland

Supporting Material

The secreted signaling protein Wnt3 is associated with membrane domains *in vivo*: a SPIM-FCS study

Xue Wen Ng[1,2], Cathleen Teh[3], Vladimir Korzh[3,4], Thorsten Wohland[1,2,4,*]

[1]Department of Chemistry, National University of Singapore, Singapore

[2]Center for BioImaging Sciences, National University of Singapore, Singapore

[3]Institute of Molecular and Cell Biology, Agency for Science, Technology and Research, Singapore

[4]Department of Biological Sciences, National University of Singapore, Singapore

Materials and Methods

Lipids, dyes and drugs

The lipids used in this study were 1,2-dioleoyl-*sn*-glycero-3-phophocholine (DOPC) and 1,2-dioleoyl-*sn*-glycero-3-phosphoglycerol (DOPG). Head group labeled rhodamine dye 1,2-dimyristoyl-*sn*-glycero-3-phosphoethanolamine-N-(lissamine rhodamine B sulfonyl) (ammonium salt) (RhoPE) was used as the fluorophore. All lipids and dyes were purchased from Avanti Polar Lipids (Alabaster, AL, USA) and prepared in chloroform. Methyl-β-cyclodextrin (mβCD) was purchased from Sigma-Aldrich (St. Louis, MO, USA) and prepared in 1 × phosphate buffered saline (PBS) for GUV measurements, 1 × Hanks' balanced salt solution (HBSS; Life Technologies, Grand Island, NY, USA) for live cell measurements and 1 × Danieau's solution (100 × Danieau's solution: 1740 mM NaCl, 21 mM KCl, 12 mM $MgSO_4 \cdot 7H_2O$, 18 mM $Ca(NO_3)_2$, 150 mM HEPES, pH 7.6) for zebrafish measurements. Cholesterol oxidase from Streptomyces sp. (Sigma-Aldrich, St. Louis, MO, USA; stock solution 50 U/mL in 50 mM potassium phosphate buffer, pH 7) (COase) was dissolved in 1 × HBSS for treatment in live cells and 1 × Danieau's solution for treatment in live zebrafish embryos. Porcupine inhibitor, C59 (500496) was purchased from Merck (Germany). 1,1'-dioctadecyl-3,3,3',3'-tetramethylindocarbocyanine perchlorate (DiI-C_{18}) purchased from Life Technologies (Grand Island, NY, USA) was used for cell membrane staining. The stock DiI-C_{18} solution was prepared in dimethyl sulfoxide (DMSO) and its concentration was calculated from the absorbance measurement in UV–Visible spectrometer (NanoDrop, Thermo Scientific, Waltham, MA, USA), assuming a molar extinction coefficient of 144,000 $M^{-1}cm^{-1}$. Ethyl 3-aminobenzoate methanesulfonate (Tricaine) was purchased from Sigma-Aldrich (St. Louis, MO, USA) and dissolved in 1 × Danieau's solution to anesthetize the zebrafish larvae before SPIM-FCS measurements.

Preparation of giant unilamellar vesicles (GUVs)

Giant unilamellar vesicles (GUVs) were prepared by the gentle hydration method (1). Briefly, calculated amounts of lipid(s) and RhoPE dye solutions were first mixed in a clean round bottom

flask and rotary evaporated (Rotavap R-210, Buchi; Switzerland) for 3 hours. The thin film of lipid left at the bottom of the round bottom flask was then resuspended gently with 2 mL of 0.5 M sucrose solution. The DOPC:DOPG (10:1) GUV solution was incubated overnight at 37 °C for GUV swelling and then stored at 4 °C. Before measurements were conducted, custom-cut No. 1 cover slips (0.13 – 0.16 mm thickness) (Marienfeld, Germany) are coated with 100 µg/mL Poly-L-Lysine solution (PLL) (Sigma-Aldrich, St. Louis, MO, USA) for GUV attachment. Next, GUVs were diluted ~20 × with 0.5 M glucose solution and added onto the PLL-coated cover slips which are then incubated for 2 h at room temperature for GUV attachment on glass. Unattached GUVs were then removed by washing with the imaging medium (1 × PBS). The cover slips were then mounted in the SPIM chamber containing 1 × PBS for SPIM-FCS measurements.

Cell culture, DiI-C_{18} staining and GFP-GPI AP transfection

SH-SY5Y cells obtained from ATCC (Manassas, VA, USA) were cultivated in DMEM medium (Dulbecco's Modified Eagle Medium; HyClone, GE Healthcare Life Sciences, South Logan, UT, USA), supplemented with 10% FBS (fetal bovine serum; HyClone, GE Healthcare Life Sciences, South Logan, UT, USA) and 1% PS (penicillin and streptomycin, PAA, Austria) at 37 °C in 5% (v/v) CO_2 humidified environment. For DiI-C_{18} staining, the stock DiI-C_{18} solution (in DMSO) was diluted to a final concentration of 50 nM with 1 × HBSS. The culture medium (DMEM, 10% FBS and 1% PS) was first removed from the 35 mm dish containing custom-cut cover slips previously seeded with cells and the cells were washed twice with 1 × HBSS before adding the 50 nM DiI-C_{18} solution. Cells were then incubated at 37 °C in 5% (v/v) CO_2 humidified environment for 25 minutes. After incubation, the cells were then rinsed with 1 × HBSS twice and placed into the SPIM chamber containing 1 × HBSS for SPIM-FCS measurements.

Green fluorescent protein-tagged glycosylphosphatidylinositol anchored protein (GFP-GPI AP) was a kind gift from John Dangerfield (Anovasia Pte Ltd, Singapore). GFP-GPI AP was transfected into live SH-SY5Y cells by electroporation using the Neon™ Transfection System from Life Technologies (Grand Island, NY, USA). SH-SY5Y cells ~90% confluent in a 25 cm^2 culture flask were washed with 1 × PBS twice and trypsinized with 0.5 mL of 1 × Trypsin solution for 1 minute at 37 °C. After trypsinization, cells were resuspended with 3.5 mL of culture medium and pelleted by centrifugation. The cell pellet was then re-suspended with 10 µL of resuspension R buffer, mixed with appropriate amount of plasmids, drawn into a 10 µL Neon transfection tip and electroporated in the Neon transfection tube containing 3 mL of electroporation E buffer with the optimized experimental conditions for SH-SY5Y cell line. After transfection, cells were plated onto a 35 mm dish containing custom-cut cover slips and grown in culture medium (DMEM and 10% FBS) at 37 °C in 5% (v/v) CO_2 humidified environment. SPIM-FCS measurements were conducted 48–60 hours post-transfection in 1 × HBSS. Transfected SH-SY5Y cells were washed twice with 1 × HBSS and filled with 1 × HBSS before measurements. For mβCD treatment, the original imaging medium (1 × HBSS) was replaced from the SPIM sample chamber with 2.5 mM mβCD dissolved in the imaging medium. For COase treatment, GFP-GPI AP transfected SH-SY5Y cells were incubated with 1 U/mL COase dissolved in 1 × HBSS for 30 minutes at 37 °C with 5% (v/v) CO_2 humidified environment. COase-treated cells on the custom-cut cover slip were then placed into the SPIM sample chamber with 1 × HBSS as the imaging medium.

Zebrafish maintenance and preparation

Transgenic lines used in this work were Tg(-8.0*cldnB*:lynEGFP), used for its weak membrane-tethered EGFP expression in the cerebellum (2), and *wnt3* promoter-driven transgenic line Tg(-4.0*wnt3*:Wnt3EGFP)^{F3}, used for its expression of functional fusion protein Wnt3-EGFP in the brain to study both Lyn-EGFP and Wnt3-EGFP diffusion properties and membrane organization by SPIM-FCS and SPIM-FCS diffusion law analysis, respectively, in the cerebellum. Transgenic adult zebrafish and embryos were maintained and obtained at the zebrafish facility in the Institute of Molecular and Cell Biology (IMCB, Singapore) and staged as described (3, 4). The Institutional Animal Care and Use Committee (IACUC) in Biological Resource Center (BRC), A*STAR Singapore, has approved the entire study (IACUC #120787). Embryos older than 30 hours post fertilization (hpf) were treated with 1-phenyl-2-thiourea (PTU; Sigma-Aldrich, St. Louis, MO, USA) to prevent the pigmentation of the embryos due to the formation of melanin.

Zebrafish embryo treatments and measurement

The zebrafish embryos were treated with 1% DMSO (control) and Porcupine inhibitor C59 (2.5 µM, 5 µM and 7.5 µM) at 36 hpf. All C59 solutions contain 1% DMSO. The zebrafish embryos were incubated in these solutions until SPIM-FCS measurements were conducted at 3 days post fertilization (dpf). mβCD treatment on the zebrafish embryos were conducted according to the protocol by Abu Siniyeh et al. (5). Briefly, 3 dpf zebrafish embryos were incubated with 2.5 mM mβCD (dissolved in 1 mL of 1 × Danieau's solution) for 40 minutes at room temperature. The embryos were then washed with 1 × PBS three times. For COase treatment, 3 dpf zebrafish embryos were incubated with 1 U/mL COase diluted in 1 × Danieau's solution (from the stock solution of 50 U/mL COase) for 40 minutes at room temperature. After treatment, the embryos were then washed thrice with 1 × PBS. Measurements were conducted on untreated and treated 3 dpf zebrafish embryos after anesthetizing them with 0.05% (w/v) Tricaine dissolved in 1 × Danieau's solution for 30 minutes. Anesthetized embryos were then mounted using 1% low melting point agarose into a thin glass capillary tube for SPIM-FCS measurements in 1 × PBS containing 0.05% (w/v) of tricaine as the imaging medium. De-yolking of both treated (7.5 µM C59) and untreated 3 dpf Wnt3-EGFP-expressing zebrafish embryos were conducted by removing the yolk of the embryos with two 27G needles, each attached to 1 mL syringes. De-yolked embryos were anesthetized with 0.05% (w/v) Tricaine dissolved in 1 × Danieau's solution for 20 minutes and mounted onto a No. 1 35 mm glass-bottom dish (MatTek Corporation, Ashland, MA, USA) using 1% low melting point agarose for confocal imaging and FCS measurements.

Confocal imaging and FCS

The confocal imaging experiments were performed in a commercial Olympus FV1200 laser scanning confocal microscope (IX83; Olympus, Singapore). The 488 nm Argon-ion multi-line laser beam (Melles Griot, Singapore) was focused on the sample by a water immersion objective (UPLSAPO, 60×, NA 1.2; Olympus, Singapore) after being reflected by a dichroic mirror (DM405/488/543/635 band pass; Olympus, Singapore) and a scanning unit. The fluorescence signal from the sample was passed through the same objective, de-scanned and finally through a 120 µm pinhole in the image plane to block the out-of-focus light and was finally recorded by the photomultiplier tube after spectrally filtered by a bandpass emission filter (BA505-605;

Olympus, Singapore). Confocal images with a field of view of 640×640 pixels and 330 nm pixel size were acquired at a rate of 200 µs/pixel.

Confocal FCS measurements were performed in the above-described confocal microscope (IX83; Olympus, Singapore) equipped with a time-resolved LSM upgrade kit (Microtime 200; PicoQuant, GmbH, Berlin, Germany). The fluorescence from the sample first passes through the 120 µm pinhole, filtered by a 513/17-25 emission filter (Semrock, Rochester, NY, USA) and finally was recorded by a single molecule avalanche photodiode (SPAD) (SPCM-AQR-14, PerkinElmer Optoelectronics, Quebec, Canada). The signals were further processed to obtain and fit the autocorrelation function (ACF) by the Symphotime 400 software (PicoQuant, GmbH, Berlin, Germany) using the following model:

$$G_{2D,2p1t}(\tau) = \frac{1}{N}\left((1-F_2)\left(1+\frac{\tau}{\tau_{D1}}\right)^{-1} + F_2\left(1+\frac{\tau}{\tau_{D2}}\right)^{-1}\right) \left(1+\left(\frac{F_{trip}}{1-F_{trip}}\right)e^{-\frac{\tau}{\tau_{trip}}}\right) + G_\infty \quad (1)$$

$$K = \frac{z_0}{\omega_0} \quad (2)$$

$$\tau_D = \frac{\omega_0^2}{4D} \quad (3)$$

where $G_{2D,2p1t}(\tau)$ is the theoretical ACF for two component (2p) 2D Brownian diffusion through a Gaussian laser profile with a triplet state contribution (1t), N is the average number of molecules in the observation volume, F_2 is the mole fraction of the second component, τ is the lag time, τ_{D1} and τ_{D2} are the diffusion times, i.e. the time taken for particles to transit the observation volume, of the first and second components respectively, K is the structure factor which defines the shape of the observation volume, F_{trip} is the fraction of the triplet state of the fluorophore, τ_{trip} is the relaxation time of the triplet state of the fluorophore, ω_0 and z_0 are the radial and axial distances of the excitation laser beam profile defined at the $1/e^2$ value of the maximum intensity at the focus of the observation volume, D is the diffusion coefficient of the respective components and G_∞ is the convergence value at infinity lag time.

Results and Discussion

SPIM-FCS performs three dimensional (3D) mapping of membrane probe diffusion

In the past we have shown that diffusion coefficient maps can be recorded in 2D samples using ITIR-FCS, and in a novel demonstration of the versatility of SPIM-FCS in mapping diffusion of fluorescent probes in 3D samples, we constructed the 2D membrane diffusion maps of a RhoPE-labeled DOPC:DOPG (10:1) GUV and a live SH-SY5Y cell labeled with DiI-C_{18}, a freely diffusing membrane marker, in a series of axial sections by means of translating the entire GUV or cell in the z-direction of the detection objective using precise microscope positioners. Integration of all the D maps from each plane of the axial sections provides a 3D view of the RhoPE and DiI-C_{18} diffusion in the membranes of the GUV and live SH-SY5Y cell respectively (Figs. S1 and S2). The simultaneous FCS measurements on all pixels in a ROI at a given plane

by SPIM-FCS to generate a *D* map outperform the sequential point-by-point FCS measurements, which require much longer measurement times, in conventional confocal FCS to generate a *D* map with the same statistics. This advantage is more pronounced when multiple planes of *D* maps are acquired to construct a 3D *D* image. Simultaneous FCS measurements of multiple points can also be achieved on a single plane by ITIR-FCS. However, ITIR-FCS measurements are restricted to the lower membrane of model lipid bilayers and live cells, close to the cover slip, due to the limited penetration depth of the evanescent wave (~100 nm) in total internal reflection (TIR) illumination that do not allow the generation of diffusion maps at multiple planes.

The step size and the number of z-stacks can be precisely selected and controlled based on the type of sample, sample size, and the light sheet thickness which dictates the smallest achievable step size by the motorized stages. In this case, step sizes of 1.5 µm were chosen to enable us to capture the membrane diffusion of RhoPE/DiI-C_{18} at various z-positions of the GUV/cell from the upper membrane (z = 0.0 µm) to the membrane boundary close to the lower membrane of the GUV/cell (z = 6.0 µm). Note that the optical sectioning ability of the light sheet illumination in SPIM allows us to conduct SPIM-FCS measurements at multiple planes without prematurely photobleaching other planes that are not focused. Figs. S1 and S2 clearly outline the overlap between the SPIM and *D* images at different z-positions on the membrane of the GUV and SH-SY5Y cell labeled with RhoPE and DiI-C_{18} respectively. The average *D* values for each plane were extracted by intensity thresholding the SPIM images to exclude the arbitrary *D* values from the background and tabulated in Table S1 in the supporting information. *D* decreases with the sections z-position from the upper membrane of the DOPC:DOPG (10:1) GUV (Fig. S1 and Table S1). As shown in Fig. S3 this z-dependence is a result of the asymmetry of the observation volume in SPIM-FCS whose extension is longer in the axial PSF (ω_z = 1280 nm) compared to the radial (ω_{xy} = 760 nm) direction (6), and the orientation of the membrane, in which the diffusion takes place, with respect to the observation volume. At the top of the vesicle the membrane is flat and spans across the radial cross section of the observation volume. In this case the smallest possible membrane area is observed. As one scans across the vesicle in z-direction the membrane is oriented increasingly along the z-direction and larger membrane patches are observed, thus increasing the average time a particle needs to pass through the observation volume. Thus the apparent diffusion coefficient measured decreases. A similar effect was earlier observed by Milon et al. via confocal FCS measurements at different positions of a GUV (7). A systematic correction for this artefact requires a precise knowledge of the membrane topology and the relative orientation between membrane and observation volume. While possible for GUVs, which possess spherical symmetry, this is more difficult for cells. Therefore, we conduct all measurements with the light sheet parallel to the membrane to be studied. A solution to this problem can be found by either recording z-stack images to determine the membrane topology or by using an isotropic observation volume (8, 9). It should be noted that for adherent cells this dependence is somewhat smaller as the cells have a more flattened geometry compared to GUVs (Fig. S2 and Table S1).

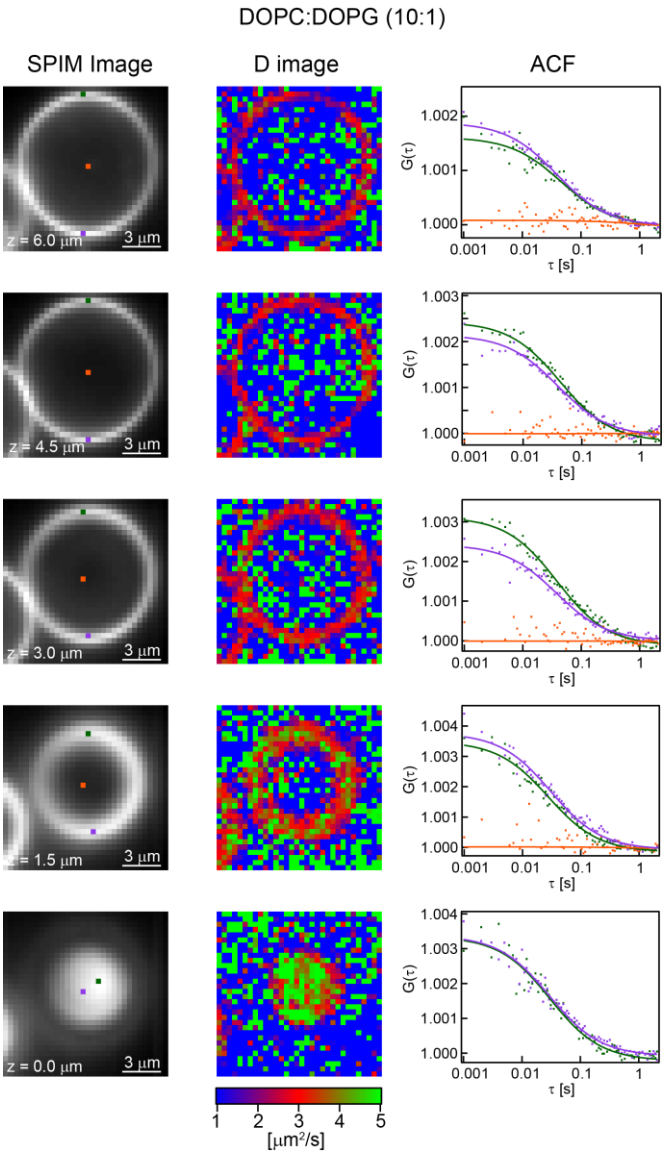

Fig. S1: 3D maps of Intensity (1st column) and *D* (2nd column) of a RhoPE-labeled DOPC:DOPG (10:1) GUV of diameter 11.2 µm. The z-positions indicate the distance from the upper membrane of the GUV. Representative ACFs (3rd column) are displayed for each z-position of their corresponding points indicated on the Intensity stack (1st column).

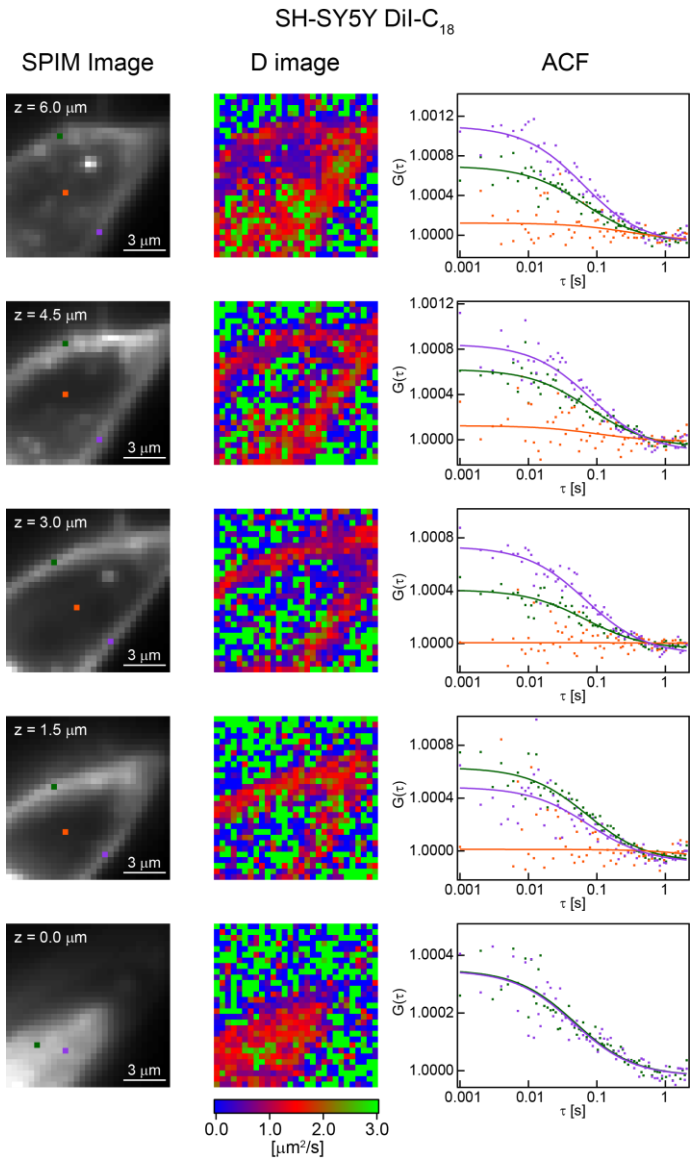

Fig. S2: 3D maps of Intensity (1st column) and *D* (2nd column) for a DiI-C_{18} labeled live SH-SY5Y cell. The z-positions indicate the distance from the upper membrane of the cell. Representative ACFs (3rd column) are displayed for each z-position of their corresponding points indicated on the Intensity stack (1st column).

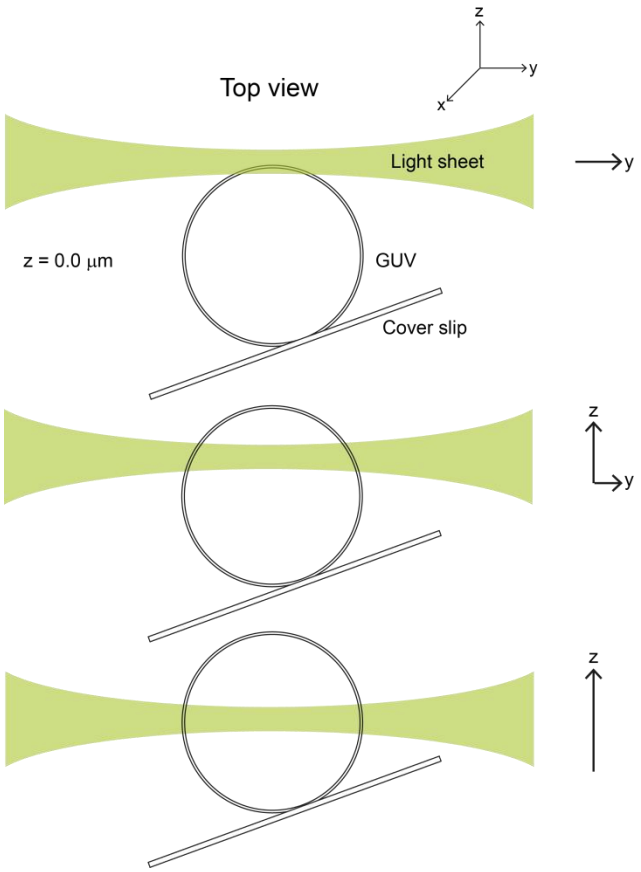

Fig. S3: Different contributions of the y- and z-components of the light sheet to the observation volume at *z*-positions from the upper membrane to the center of the GUV as seen from the top view of the SPIM chamber.

Table S1: *z* dependence of *D* for RhoPE-labeled DOPC:DOPG (10:1) GUV and live SH-SY5Y cell membranes labeled with DiI-C_{18} and GFP-GPI AP respectively. Percentage change in *D* is given with respect to the *D* of the upper membrane (z = 0.0 µm) and calculated as $\Delta D/D_{z=0} \times 100\%$. *D* values are given in mean ± SD.

Sample	*z*-position from upper membrane [µm]	*D* [µm^2/s]	% change in *D*
DOPC:DOPG (10:1) (RhoPE)	0.0	4.04 ± 1.18	0.0
	1.5	3.47 ± 0.90	- 14.0
	3.0	2.91 ± 0.85	- 28.0
	4.5	2.55 ± 0.95	- 36.9
	6.0	2.47 ± 0.84	- 38.9
SH-SY5Y (DiI-C_{18})	0.0	1.95 ± 0.73	0.0
	1.5	2.02 ± 0.69	+ 3.6
	3.0	1.77 ± 0.74	- 9.2
	4.5	1.82 ± 0.63	- 6.7
	6.0	1.94 ± 0.80	- 0.5
SH-SY5Y (GFP-GPI AP)	0.0	0.32 ± 0.10	0.0
	1.5	0.32 ± 0.12	0.0
	3.0	0.28 ± 0.13	- 12.5

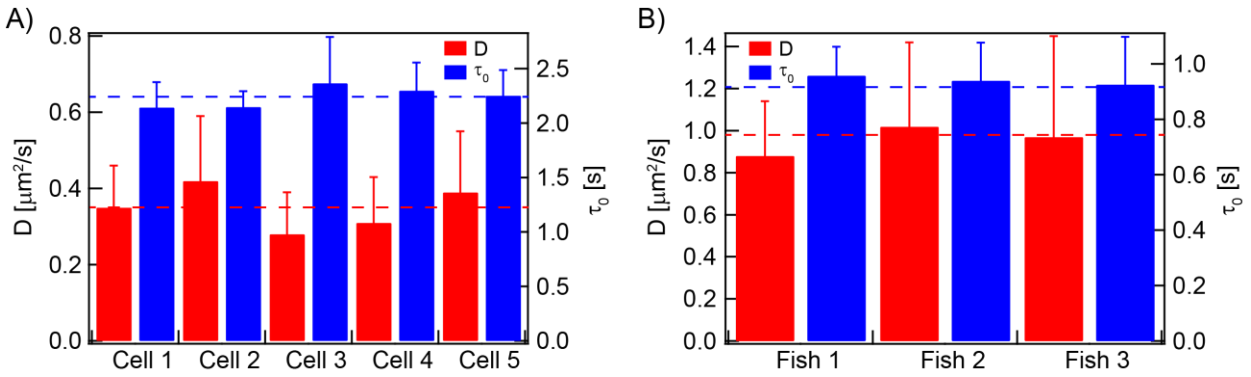

Fig. S4: Values of D and τ_0 across various measurements for A) GFP-GPI AP labeled SH-SY5Y cell membranes and B) cerebellar cell membranes of live Wnt3-EGFP transgenic zebrafish embryos. The dotted lines represent the average D (red) and τ_0 (blue) values across all measurements.

Margin of error for free diffusion of the SPIM-FCS diffusion law intercept (τ_0) and comparison of τ_0 values between SPIM-FCS and ITIR-FCS diffusion laws

The margin of error of the SPIM-FCS diffusion law intercept where processes exhibit free diffusion was determined by conducting SPIM-FCS diffusion law analysis on the upper membrane of a freely-diffusing model membrane, RhoPE-labeled DOPC:DOPG (10:1) GUV. Overall, 17 measurements were conducted on 11 GUVs and their τ_0 values were found to lie within ± 0.2 s (Fig. S5A). Therefore, τ_0 values which fall within the range of ± 0.2 s were designated as free diffusion.

Next, we compared the τ_0 values obtained from the FCS diffusion law analyses of SPIM-FCS and ITIR-FCS on similar samples to test the robustness of the SPIM-FCS diffusion law in distinguishing membrane heterogeneity. The τ_0 values of both RhoPE-labeled DOPC:DOPG (10:1) GUVs and DiI-C_{18} labeled SH-SY5Y cells demonstrated free diffusion, which is consistent with their respective localization on the membrane (Fig. S5B, C, D, Table S2). ITIR-FCS diffusion law analyses also yielded τ_0 values within its margin of error of ± 0.1 s (i.e. free diffusion) for DOPC supported lipid bilayers and DiI-C_{18} labeled HeLa and CHO-K1 cells (Table S2), further supporting the applicability of the SPIM-FCS diffusion law. The margin of errors of the τ_0 values for SPIM-FCS and ITIR-FCS diffusion laws vary due to their different pixel sizes (SPIM-FCS: 400 nm, ITIR-FCS: 240 nm) and point spread functions (PSFs) (10, 11). It was earlier found that pixel size and PSF affect the precision of the FCS diffusion law intercept (12). The larger pixel size and PSF of the SPIM optical system decreases the precision of τ_0 for SPIM-FCS diffusion law and raises its margin of error in comparison to that of the ITIR-FCS diffusion law (± 0.2 s for SPIM-FCS vs ± 0.1 s for ITIR-FCS). In the case of raft marker GFP-GPI AP, both SPIM-FCS and ITIR-FCS diffusion law intercepts were well above their respective margin of errors, indicating domain confinement of the probe for all cases (Fig. S5B, C, D, Table S2). The difference in the absolute τ_0 values of GFP-GPI AP obtained from SPIM-FCS and ITIR-FCS diffusion laws thus could be due to the different cell lines used and the influence of pixel size and PSF as mentioned earlier. This demonstrates the capability of the SPIM-FCS diffusion law to accurately determine the type of membrane organization of a given probe.

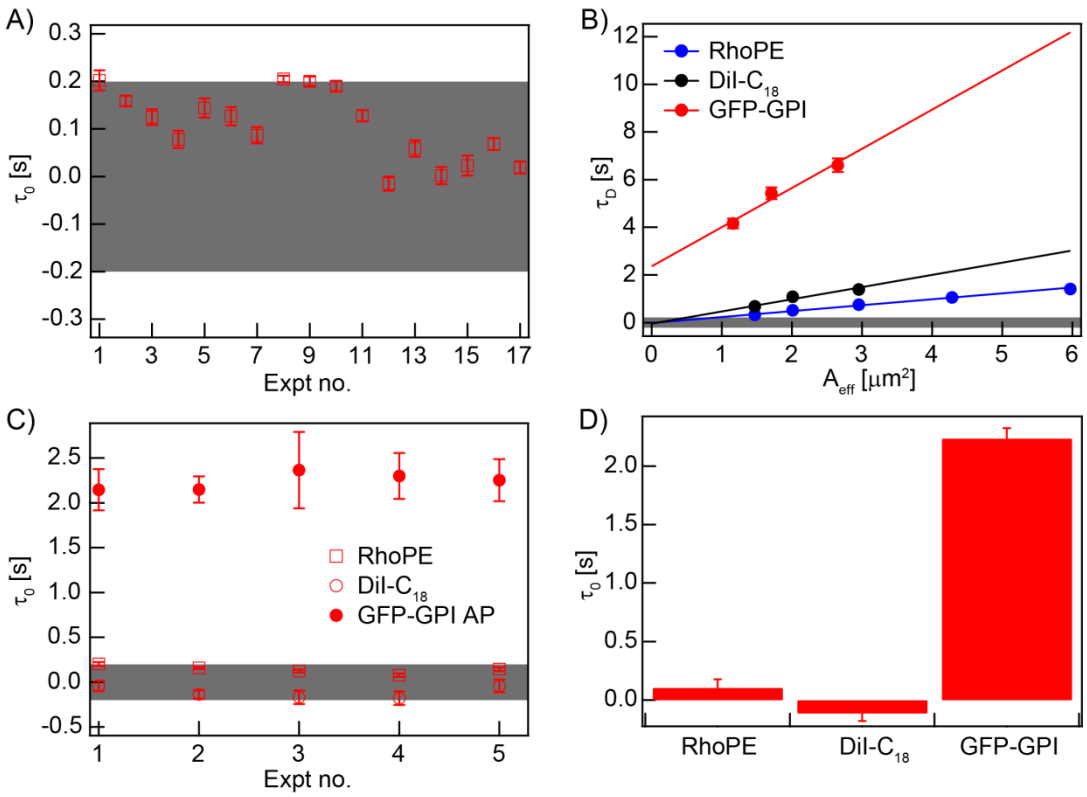

Fig. S5: Proof of the SPIM-FCS diffusion law on model and live SH-SY5Y cell membranes. A) SPIM-FCS diffusion law intercepts of the upper membrane of freely-diffusing RhoPE-labeled DOPC:DOPG (10:1) GUV for 17 measurements (11 GUVs, 1147 ACFs). The grey region indicates the margin of error (± 0.2 s) of τ_0 values for which processes demonstrate free diffusion when investigated by SPIM-FCS. B) Representative SPIM-FCS diffusion law plots of the upper membranes of RhoPE-labeled DOPC:DOPG (10:1) GUV, DiI-C_{18} and GFP-GPI AP labeled SH-SY5Y cells. C) τ_0 values for 5 measurements of RhoPE-labeled DOPC:DOPG (10:1) GUVs, DiI-C_{18} and GFP-GPI AP labeled SH-SY5Y cells respectively. D) Average τ_0 values for RhoPE-labeled DOPC:DOPG (10:1) GUVs (11 GUVs, 17 measurements, 1147 ACFs), DiI-C_{18} (3 cells, 5 measurements, 337 ACFs) and GFP-GPI AP (5 cells, 5 measurements, 446 ACFs) labeled SH-SY5Y cells.

Table S2: Comparison of SPIM-FCS and ITIR-FCS diffusion law intercepts for various probes in model and live cell membranes. Data are represented as mean ± SD of number of measurements.

Fluorophore (Sample)	**Measurement mode**	**τ_0 [s]**	**Diffusion mode**	$N_{GUVs/cells}$	$N_{measurement}$	N_{ACFs}	**Ref.**
RhoPE (DOPC:DOPG (10:1))	SPIM-FCS	0.11 ± 0.07	Free	11	17	1147	Current
RhoPE (DOPC)	ITIR-FCS	-0.04 ± 0.26	Free	-	-	-	(11)
DiI-C_{18} (SH-SY5Y)	SPIM-FCS	-0.11 ± 0.07	Free	3	5	337	Current
DiI-C_{18} (HeLa)	ITIR-FCS	within ± 0.1	Free	-	-	-	(13)
DiI-C_{18} (CHO-K1) (14)	ITIR-FCS	-0.05 ± 0.01	Free	-	-	-	(14)
GFP-GPI AP (SH-SY5Y)	SPIM-FCS	2.24 ± 0.09	Confined	5	5	446	Current
GFP-GPI AP (HeLa)	ITIR-FCS	3.96 ± 0.17	Confined	-	-	-	(13)
GFP-GPI AP (CHO-K1)	ITIR-FCS	1.27 ± 0.05	Confined	-	-	-	(14)

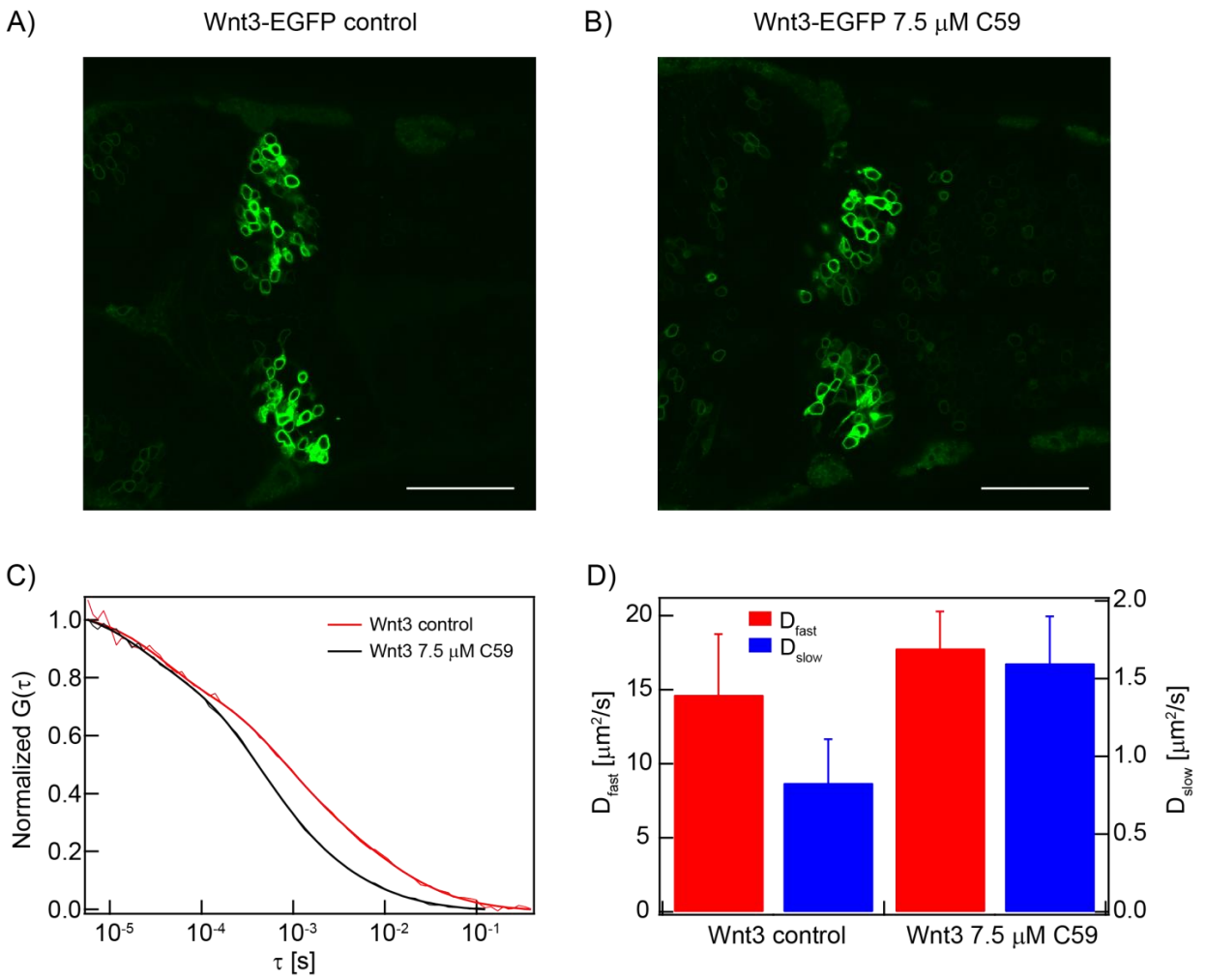

Fig. S6: Confocal imaging and FCS measurements of de-yolked Tg(-4.0*wnt3*:Wnt3EGFP)[F3] Wnt3-EGFP-expressing 3 dpf zebrafish embryos. Confocal images of the cerebellum of de-yolked Wnt3-EGFP-expressing embryos A) without treatment (control) and B) with 7.5 µM C59 treatment. All scale bars are 50 µm. C) Representative normalized ACFs of Wnt3-EGFP dynamics on the cerebellar cell membranes of untreated (control) and 7.5 µM C59 treated embryos. D) Average D_{fast} and D_{slow} values for Wnt3-EGFP measured on the cerebellar cell membranes for control (3 fishes, 4 cells, 5 ACFs) and 7.5 µM C59 treated (3 fishes, 5 cells, 5 ACFs) embryos.

Supporting References

1. Morales-Penningston, N.F., J. Wu, E.R. Farkas, S.L. Goh, T.M. Konyakhina, J.Y. Zheng, W.W. Webb, and G.W. Feigenson. 2010. GUV Preparation and Imaging: Minimizing artifacts. Biochim. Biophys. Acta. 1798: 1324–1332.

2. Haas, P., and D. Gilmour. 2006. Chemokine Signaling Mediates Self-Organizing Tissue Migration in the Zebrafish Lateral Line. Dev. Cell. 10: 673–680.

3. Kimmel, C.B., W.W. Ballard, S.R. Kimmel, B. Ullmann, and T.F. Schilling. 1995. Stages of embryonic development of the zebrafish. Dev. Dyn. 203: 253–310.

4. Westerfield, M. 2000. The Zebrafish Book. A Guide for the Laboratory Use of Zebrafish (Danio rerio). 4th ed. University of Oregon Press, Eugene.

5. Abu-Siniyeh, A., D.M. Owen, C. Benzing, S. Rinkwitz, T.S. Becker, A. Majumdar, and K. Gaus. 2016. The aPKC/Par3/Par6 Polarity Complex and Membrane Order Are Functionally Interdependent in Epithelia During Vertebrate Organogenesis. Traffic. 17: 66–79.

6. Krieger, J.W., A.P. Singh, C.S. Garbe, T. Wohland, and J. Langowski. 2014. Dual-color fluorescence cross-correlation spectroscopy on a single plane illumination microscope (SPIM-FCCS). Opt. Express. 22: 2358–2375.

7. Milon, S., R. Hovius, H. Vogel, and T. Wohland. 2003. Factors influencing fluorescence correlation spectroscopy measurements on membranes: Simulations and experiments. Chem. Phys. 288: 171–186.

8. Galland, R., G. Grenci, A. Aravind, V. Viasnoff, V. Studer, and J.-B. Sibarita. 2015. 3D high- and super-resolution imaging using single-objective SPIM. Nat. Methods. 12: 641–644.

9. Capoulade, J., M. Wachsmuth, L. Hufnagel, and M. Knop. 2011. Quantitative fluorescence imaging of protein diffusion and interaction in living cells. Nat. Biotechnol. 29: 835–839.

10. Singh, A.P., J.W. Krieger, J. Buchholz, E. Charbon, J. Langowski, and T. Wohland. 2013. The performance of 2D array detectors for light sheet based fluorescence correlation spectroscopy. Opt. Express. 21: 8652–8668.

11. Bag, N., J. Sankaran, A. Paul, R.S. Kraut, and T. Wohland. 2012. Calibration and limits of camera-based fluorescence correlation spectroscopy: A supported lipid bilayer study. ChemPhysChem. 13: 2784–2794.

12. Sankaran, J., N. Bag, R.S. Kraut, and T. Wohland. 2013. Accuracy and precision in camera-based fluorescence correlation spectroscopy measurements. Anal. Chem. 85: 3948–3954.

13. Bag, N., D.H.X. Yap, and T. Wohland. 2014. Temperature dependence of diffusion in model and live cell membranes characterized by imaging fluorescence correlation spectroscopy. Biochim. Biophys. Acta. 1838: 802–813.

14. Bag, N., S. Huang, and T. Wohland. 2015. Plasma Membrane Organization of Epidermal Growth Factor Receptor in Resting and Ligand-Bound States. Biophys. J. 109: 1925–1936.